

## Time-resolved Stokes shift in proteins with continuum model: Slow dynamics in proteins

Rong Rujkorakarn<sup>a</sup>, Nadtanet Nunthaboot<sup>b</sup>, Fumio Tanaka<sup>c,\*</sup>, Pimchai Chaiyen<sup>c</sup>,  
Haik Chosrowjan<sup>d,\*\*</sup>, Seiji Taniguchi<sup>d</sup>, Noboru Mataga<sup>d</sup>

<sup>a</sup> Department of Physics, Faculty of Science, Maharakham University, Maharakham 44150, Thailand

<sup>b</sup> Department of Chemistry, Faculty of Science, Maharakham University, Maharakham 44150, Thailand

<sup>c</sup> Department of Biochemistry and Center of Excellence in Protein Structure and Function, Faculty of Science, Mahidol University, Bangkok 10400, Thailand

<sup>d</sup> Institute for Laser Technology, Utsubo-Hommachi 1-8-4, Nishiku, Osaka 550-0004, Japan

### ARTICLE INFO

#### Article history:

Received 3 March 2010

Received in revised form 23 June 2010

Accepted 20 July 2010

Available online 27 July 2010

#### Keywords:

Tryptophan

Protein

Time-resolved Stokes shift

Flavin

C1 protein

Theoretical analyses

Continuum model

### ABSTRACT

Reported time-resolved Stokes shifts (TRSS) of free tryptophan (Trp) and free *p*-coumaric acid (CA) in water, and Trp in monellin, apomyoglobin, and isoalloxazine (Iso) of flavin mononucleotide (FMN) in the reductase component (C<sub>1</sub> protein) of *p*-hydroxyphenylacetate hydroxylase were analyzed with continuum model. All unknown parameters of these systems in the theoretical equations were determined to obtain the best fit between the observed and calculated TRSS, according to a non-linear least square method. TRSS of free Trp at 295 K was also analyzed with four sets of reported dielectric constants and solvent relaxation times of water. Agreement between the observed and calculated TRSS of the free Trp was excellent. In CA the calculated TRSS could satisfactorily reproduce the observed one. Frequency-dependent dielectric constants of Trp in the proteins and Iso in C<sub>1</sub> protein were expressed with 2- and 3-relaxation times. Static dielectric constant,  $\epsilon_0$ , intermediate permittivity,  $\epsilon_1$ , dielectric constant of Iso,  $\epsilon_c$ , 2-relaxation times,  $\tau_1$  and  $\tau_2$ ,  $\mu_e$  and  $D_0$  in the 2-relaxation time analyses were determined by the best-fit procedures. Agreements between the observed and calculated TRSS of Trp in native, denatured monellins, apomyoglobin, and Iso in C<sub>1</sub> protein were excellent. No further improvements were obtained with 3-relaxation time analyses. Origin of the slow decaying component of TRSS in apomyoglobin was interpreted with continuum model and compared with molecular dynamics (MD) simulation model and a continuum model by Halle and Nilsson [J. Phys. Chem. B 113 (2009) 8210]. Frozen states revealed with MD model were reproduced with the 3-relaxation time analysis.

© 2010 Elsevier B.V. All rights reserved.

### 1. Introduction

Since seminal theoretical reports on Stokes shift (SS) [1,2], dipole moments of dyes in the excited states can be experimentally determined under steady-state excitation. Theoretical expressions of time-resolved Stokes shift (TRSS) was first derived by Bagchi et al. based on continuum theory [3,4]. After these reports a number of investigations on solvation dynamics of organic dyes have been carried out experimentally by means of time-resolved fluorescence spectroscopy [5–11]. Molecular dynamics simulations have also been applied to TRSS [12–14].

Rotational motion of solute is related both to TRSS [1] and time-resolved fluorescence anisotropy (TRAN). Dielectric friction given by Nee and Zwantig [15] was introduced into rotational motion of solute molecules, and unified expressions of TRSS and TRAN were derived using the continuum theory [16]. The theory was applied to TRSS and TRAN of a rod-like molecule of *p*-cyano-*p*'-methoxydiphenylethin [17]. Both of the TRSS and TRAN were analyzed using common parameters.

In the last decade, solvation dynamics of chromophores at water–protein interfaces have been investigated by many research groups [18–22]. TRSS of the chromophores displayed unusual slow decaying components, which have never been found in solution. Intrinsic fluorophore of tryptophan (Trp) located at protein–water interface also exhibited slow decaying component in many proteins [23–33]. Peon et al. [25] demonstrated that a decay constant of the slow decaying component in TRSS of Trp3 in monellin was 16 ps, which was 12 times longer than that of the faster component. Origin of the slow component was explained in terms of the dynamical exchange of water molecules between free and

\* Corresponding author. Tel.: +66 858527182.

\*\* Corresponding author.

E-mail addresses: [fukoh2003@yahoo.com](mailto:fukoh2003@yahoo.com) (F. Tanaka),  
[haik@ilt.or.jp](mailto:haik@ilt.or.jp) (H. Chosrowjan).

immobilized water molecules at the protein surface. Nilsson and Halle [27] interpreted the slow component of their TRSS data of Trp3 in monellin as a reflection of protein dynamics and the self-motion of Trp3 according to its molecular dynamics (MD) simulation. Li et al. [30] obtained 5 ps and 87 ps correlation times of Trp7 in apomyoglobin. They interpreted the TRSS data by MD study that the initial dynamics in a few picoseconds represents fast local motions such as reorientations and translations of hydrating water molecules, followed by the slow relaxation involving strongly coupled water–protein motions. Golosov and Karplus [31] also supported the concept of coupling of the hydration with protein conformational dynamics for the longer correlation time by MD. Li et al. [30,32] found by MD that protein flexibility is required to observe the slow component of Trp7 in apomyoglobin. More recently Halle and Nilsson [33] have claimed that the slow relaxation in TRSS can be explained by solvent polarization mechanism, with no need to invoke slow water motions or dynamic coupling with protein motions, using continuum model.

Recently, we have shown for the first time for flavoproteins that TRSS of FMN in the reductase component ( $C_1$ ) of *p*-hydroxyphenylacetate hydroxylase ( $C_1$  protein), displayed bi-phase behavior in the spectral correlation function with 0.455 ps and 250 ps of the correlation times [34], which are similar to Trp in monellin and apomyoglobin, though the longer component was much longer than those of Trp in proteins. In the present work we have analyzed TRSS of free Trp [25,35] and free CA [34] in water and Trp in native and denatured monellin [25], in apomyoglobin [30], and Iso in  $C_1$  protein [34], using expressions obtained by the continuum model [16,17]. Relationship between the continuum model and the MD model was discussed for the slow decaying components in TRSS of proteins.

## 2. Methods of analyses

### 2.1. MO calculation

Dipole moments of a solute in the ground and excited states were calculated by a semi-empirical molecular orbital method (PM3) with a software package of WinMOPAC (Fujitsu, Japan). Solvent effect was taken into account with EPS key word (visit for meaning of the keyword: <http://openmopac.net/>). Molecular sizes of chromophores were also determined with PM3.

### 2.2. Continuum theory of TRSS

Frequency-dependent dielectric constant with 2- and 3-relaxation times are expressed by Eq. (1):

$$\varepsilon(\omega) = \varepsilon + (\varepsilon_0 - \varepsilon) \sum_{j=1}^n \frac{g_j}{1 - i\omega\tau_j} \quad (1)$$

Here  $n$  (=2 and 3) is number of relaxation times,  $\omega$  is frequency of an external electric field,  $\tau_j$   $j$ th relaxation time of solvent, and  $g_j$  fraction of  $j$ th relaxation time.

$$\sum_{j=1}^n g_j = 1$$

$g_1 = (\varepsilon_0 - \varepsilon_1)/(\varepsilon_0 - \varepsilon)$  and  $g_2 = (\varepsilon_1 - \varepsilon)/(\varepsilon_0 - \varepsilon)$ , when  $n=2$ ,  $g_1 = (\varepsilon_0 - \varepsilon_1)/(\varepsilon_0 - \varepsilon)$ ,  $g_2 = (\varepsilon_1 - \varepsilon_2)/(\varepsilon_0 - \varepsilon)$  and  $g_3 = (\varepsilon_2 - \varepsilon)/(\varepsilon_0 - \varepsilon)$ , when  $n=3$ .  $\varepsilon_0$  and  $\varepsilon$  are static and optical dielectric constants of a solvent, respectively, and  $\varepsilon_1$  and  $\varepsilon_2$  intermediate permittivities.

TRSS with two relaxation times can be described by Eq. (2):

$$SS_2(t) = C_{F2}(\mu_e^2 + \mu_g^2 - 2\mu_e\mu_g \cos \theta) \sum_{i=1}^3 \sum_{j=1}^2 \frac{C_{Ai}C_{Bj}}{X_{Ai} + X_{Bj}} \times \exp\{-(X_{Ai} + X_{Bj})t\} \quad (2)$$

Coefficients and rate constants in Eq. (2) are given in Supplemental Material A.

TRSS with three relaxation times is expressed as in Eq. (3):

$$SS_3(t) = C_{F3}(\mu_e^2 + \mu_g^2 - 2\mu_e\mu_g \cos \theta) \sum_{i=1}^4 \sum_{j=1}^3 \frac{C_{Ai}C_{Bj}}{X_{Ai} + X_{Bj}} \times \exp\{-(X_{Ai} + X_{Bj})t\} \quad (3)$$

Coefficients and rate constants are described in Supplemental Material B.

### 2.3. Determination of unknown parameters containing in the theories of TRSS

Physical constants of Trp and CA are listed in Table S1 (Supplemental Material C). Decay parameters of Sobs( $t$ ) for free Trp reported by Shen and Knutson [35] and Peon et al. [25], and for CA reported by Chosrowjan et al. [34], are also listed in Table S1 (Supplemental Material C). Dielectric constants and solvent relaxation times of water were reported by several groups [36–39]. Frequency-dependent dielectric constants were expressed with two relaxation times. These physical constants are listed in Table S2 (Supplemental Material C).

Deviation between  $SS_2(t)$  and the observed SS in water, and its  $\chi^2$  are expressed by Eqs. (4) and (5):

$$DevS(t_i) = \frac{SS_2(t_i) - Sobs(t_i)}{\sqrt{SS_2(t_i)}} \quad (4)$$

$$\chi^2 = \frac{1}{N_S} \sum_{i=1}^{N_S} \{DevS(t_i)\}^2 \quad (5)$$

$\mu_e$ ,  $\mu_g$ ,  $\varepsilon_c$  and  $D_0$  were determined to obtain the minimum value of  $\chi^2$  with using all sets of physical constants reported [36–39]. TRSS does not depend on  $D_Z$  [16].

We do not have any information on physical constants of solvents in proteins. Firstly the observed TRSS data were analyzed using the frequency-dependent dielectric constant with two relaxation times [ $n=2$  in Eq. (1)]. In this analysis  $\varepsilon_0$ ,  $\varepsilon_1$ ,  $\varepsilon_c$ ,  $D_0$ ,  $\mu_e$ ,  $\tau_1$ , and  $\tau_2$  (see the meaning of these constants at Supplemental Material A) were varied to obtain the minimum value of  $\chi^2$  in Eq. (5). Secondly the data were analyzed with three relaxation times [ $n=3$  in Eq. (1)]. In this analysis Eq. (6) was used for the calculation of  $\chi^2$ .

$$DevS(t_i) = \frac{SS_3(t_i) - Sobs(t_i)}{\sqrt{SS_3(t_i)}} \quad (6)$$

In this analysis  $\varepsilon_0$ ,  $\varepsilon_1$ ,  $\varepsilon_2$ ,  $\varepsilon_c$ ,  $D_0$ ,  $\mu$ ,  $\tau_1$ ,  $\tau_2$  and  $\tau_3$  were unknown parameters (see the meaning of these parameters at Supplemental Material B). In all analyses described above these unknown parameters were determined at a certain value of  $D_0$ , which was sequentially varied till the values of  $\chi^2$  attained the minimum [16].  $\varepsilon=4$  was used for all analyses.

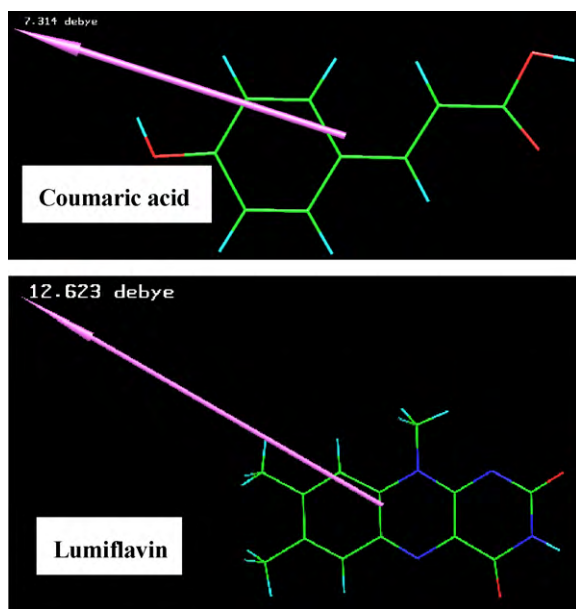


**Fig. 1.** Dipole moment of chromophores in the excited state obtained by MO method. O, C, and H atoms are indicated by red, green and blue colors. Magnitude of the dipole moments were 7.31 D in CA in water, and 12.6 D in Lf in water. The values were obtained by a semi-empirical MO method of PM3. (For interpretation of the references to color in this figure legend, the reader is referred to the web version of this article.)

### 3. Results

#### 3.1. Directions of dipole moments of chromophores in the excited states obtained by MO

Directions of dipole moments of chromophores in the excited states studied in the present work were obtained by PM3 method and are shown in Fig. 1. Theoretical dipole moments and the other physical constants are listed in Table S1. The dipole moments in the excited states were 18.5 D in Trp of zwitterions form, and 7.3 D in CA and 12.6 D in Lf in water. A dipole moment of 3-methylindole in water was 5.73 D. Chromophore of Trp in proteins was assumed

to be 3-methylindole. It was also assumed that directions of these dipole moments do not alter with solvent polarity.

#### 3.2. TRSS of Trp and CA in water

TRSS of Trp in water was reported in sub-picosecond time domain by Shen and Knutson [35] and Peon et al. [25]. Stokes shift,  $SS_2(0) - SS_2(\infty)$ , was 0.412 kK ( $1000 \text{ cm}^{-1}$ ) [35] and the decay constants [25]  $\varphi_1$  (fraction  $\alpha_1$ ) and  $\varphi_2$  (fraction  $\alpha_2$ ) were 0.180 ps (0.2) and 1.11 ps (0.8), respectively. Physical constants of Trp and water used for the analysis are listed in Tables S1 and S2 (Supplemental Material C), respectively. Dielectric constants and relaxation times of water were reported by four research groups [36–39]. Relaxation process of water can be expressed by two relaxation times as listed in Table S2. Dependence of  $SS_2(t)$  on the rotational diffusion coefficient of solute was very little. Therefore, it was difficult to obtain reasonable values of  $D_0$ , when it was included in the best-fit procedure like other unknown parameters.  $D_{\text{stick}}$  and  $D_{\text{slip}}$  were obtained from hydrodynamic constants of water and molecular size of the symmetry top solute [5] and used as  $D_0$ . Theoretical value of  $\mu_g$  obtained by PM3 was also used for the analysis, since TRSS depends on  $(\mu_e - \mu_g)^2$ , where the dipole moments are vectors. It is quite difficult to determine these dipole moments separately. These values are listed in Tables S1 and S2. Fig. 2 shows TRSS of Trp in water. Agreement between the observed and calculated  $SS_2(t)$  was optimum when dielectric constants and relaxation times reported by Kindt and Schmuttenmaer [37] were used, and stick model for the rotational diffusion coefficient.  $\mu_e$  and  $\varepsilon_c$  were obtained to be 20.2 D and 31.4, respectively. Theoretical value of  $\mu_e$  was 18.5 D. Dipole moments of free tryptophan in water were much larger than 3-methylindole because of its side chain. Calculated Stokes shift,  $SS_2(0) - SS_2(\infty)$ , was 0.415 kK, while 0.412 kK in the observed one [35]. Table 1 lists the best-fit parameters with Model A, B, C and D using  $D_{\text{stick}}$  or  $D_{\text{slip}}$ . The best-fit values of  $\mu_e$  and  $\varepsilon_c$ , and also  $\chi^2$  did not differ much when  $D_{\text{stick}}$  or  $D_{\text{slip}}$  was used. The values of  $\varepsilon_c$  and  $\chi^2$  were, however, markedly dependent on the Model A to D, while  $\mu_e$  did not change much with the calculated diffusion coefficient and the model employed. Model B was best among the four, as judged from  $\chi^2$ .

Fig. 3 shows TRSS of CA in water. The observed decay parameters were  $\varphi_1 = 0.053 \text{ ps}$  (14%) and  $\varphi_2 = 0.64 \text{ ps}$  (86%) [34] as shown in

**Table 1**  
Best-fit parameters of TRSS of Trp and CA in water<sup>a</sup>.

Chromophore	Method <sup>b</sup>	Diffusion coefficient	$SS_2(0) - SS_2(\infty)^c$ (kK)		Best-fit parameter		$\chi^2^d$ ( $\times 10^{-5}$ )
			Obs	Calc	$\mu_e$ (D)	$\varepsilon_c$	
Trp	A	Stick	0.412	0.444	20.3	31.5	26.1
		Slip	0.412	0.444	20.3	31.8	25.8
	B	Stick	0.412	0.415	20.2	31.4	0.162
		Slip	0.412	0.414	20.2	31.6	0.164
	C	Stick	0.412	0.372	20.9	24.6	8.49
		Slip	0.412	0.372	20.9	24.8	8.50
	D	Stick	0.412	0.408	20.0	35.7	0.444
		Slip	0.412	0.412	20.0	35.9	0.451
CA	A	Stick	1.300	1.471	8.61	31.6	609
		Slip	1.300	1.470	8.61	31.7	607
	B	Stick	1.300	1.452	10.1	22.3	121
		Slip	1.300	1.452	10.1	22.4	120
	C	Stick	1.300	1.239	11.0	19.2	137
		Slip	1.300	1.239	11.0	19.3	137
	D	Stick	1.300	1.418	9.01	29.2	91.4
		Slip	1.300	1.417	9.00	29.3	91.2

<sup>a</sup> Physical constants of solutes are listed in Table S1 in Supplemental Material C, respectively. Temperature was 295 K, and  $\eta$  of water 0.958 (mPas). Theoretical values were used for  $\mu_g$  and rotational diffusion coefficient of solute ( $D_{\text{stick}}$  or  $D_{\text{slip}}$ ; see Table S1).

<sup>b</sup> Dielectric constants and relaxation times reported by four groups are listed in Table S2.

<sup>c</sup>  $SS_2(t)$  is given by Eq. (2).

<sup>d</sup>  $\chi^2$  is given by Eq. (4).

**Table 2**  
TRSS parameters for proteins with two relaxation times<sup>a</sup>.

System (fluorophore)	Best-fit parameter										$\chi^2$ <sup>d</sup>		
	$\varepsilon_0$	$\varepsilon_1$	$\varepsilon_c$	$D_0$ (s <sup>-1</sup> )	$\mu_e$ (D)	$\tau_1$ (ps) (g <sub>1</sub> )	$\tau_2$ (ns) (g <sub>2</sub> )	$SS_2(0) - SS_2(\infty)$ (kK)	$\varphi_1$ <sup>b</sup> (ps) ( $\alpha_1$ <sup>c</sup> )	$\varphi_2$ <sup>b</sup> (ps) ( $\alpha_2$ <sup>c</sup> )		Calc	Obs
Native monellin <sup>e</sup> (3-methylindole)	78.4	6.76	4.51	$1.86 \times 10^7$	9.86	2.17 (0.038)	0.161 (0.962)	0.96	1.3 (0.46)	16 (0.54)	16.0 (0.540)	16.0 (0.540)	6.68 × 10 <sup>-17</sup>
Denatured monellin <sup>e</sup> (3-methylindole)	73.3	11.1	4.44	$1.0 \times 10^5$	9.92	9.70 (0.102)	0.318 (0.898)	0.96	3.5 (0.72)	56 (0.28)	56.0 (0.280)	56.0 (0.280)	1.40 × 10 <sup>-24</sup>
Apomyoglobin <sup>f</sup> (3-methylindole)	78.0	6.18	5.68	$1.00 \times 10^6$	8.01	7.42 (0.030)	0.945 (0.970)	0.660	5.0 (0.367)	87 (0.632)	87.0 (0.633)	87.0 (0.633)	1.87 × 10 <sup>-19</sup>
C1 protein <sup>g</sup> (lumiflavin)	77.7	20.4	8.36	$1.30 \times 10^5$	23.0	1.91 (0.222)	0.912 (0.778)	2.262	0.455 (0.816)	250 (0.184)	250 (0.184)	250 (0.184)	4.64 × 10 <sup>-23</sup>

<sup>a</sup>  $\varepsilon_0, \varepsilon_1, \varepsilon_c, D_0, \mu_e, \tau_1$  and  $\tau_2$  were varied so as to obtain best fit between the observed and calculated TRSS. The calculated dipole moment of 3-methylindole (Table S1 in Supplemental Material C) in the ground state was used as  $\mu_g$ .

<sup>b</sup> Observed and calculated decay constants of  $SS_2(t)$ .

<sup>c</sup> Fractions of the decay constants.

<sup>d</sup>  $\chi^2$  given by Eq. (4).

<sup>e</sup> Experimental data were taken from Ref. [25].

<sup>f</sup> Experimental data were taken from Ref. [35].

<sup>g</sup> Experimental data were taken from Ref. [34].

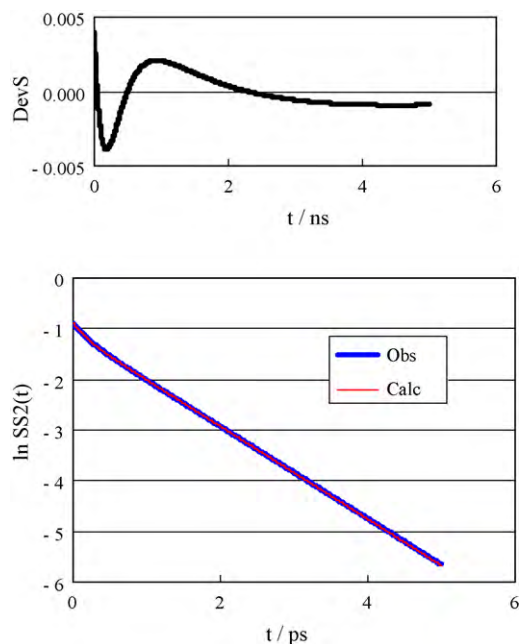


**Fig. 2.** TRSS of Trp in water.  $SS_2(t)$  is described by Eq. (2) and expressed in kK unit. The observed TRSS was taken from Refs. [25,35].  $\mu_e$  and  $\varepsilon_c$  were changed so as to obtain the minimum value of  $\chi^2$ . Theoretical values were used for  $\mu_g$  and rotational diffusion coefficient of solute ( $D_{stick}$  or  $D_{slip}$ ; see Table 1). The best fit was obtained with Model B (see Table 2) with  $D_{stick}$  all in the four models. The value of  $\chi^2$  was  $1.62 \times 10^{-6}$ . The other parameters obtained by the best-fit procedure are listed in Table 1. Upper panel shows deviations given by Eq. (4). Temperature was 295 K.

**Table S1.** The best fit was obtained when Model D with  $D_{slip}$  was used. The values of  $\mu_e$  and  $\varepsilon_c$  at the best fit were 9.00 D and 29.3 as listed in Table 1. Again these values did not differ much when  $D_{stick}$  or  $D_{slip}$  was used. Theoretical value of  $\mu_e$  was 7.31 D. The values  $\mu_g$  and  $D_{slip}$  of CA were 3.95 D and  $1.47 \text{ ns}^{-1}$ , respectively. The observed and calculated values of  $SS_2(0) - SS_2(\infty)$  were 1.3 kK [34] and 1.42 kK, respectively. Agreement between the observed and calculated TRSS was very good.

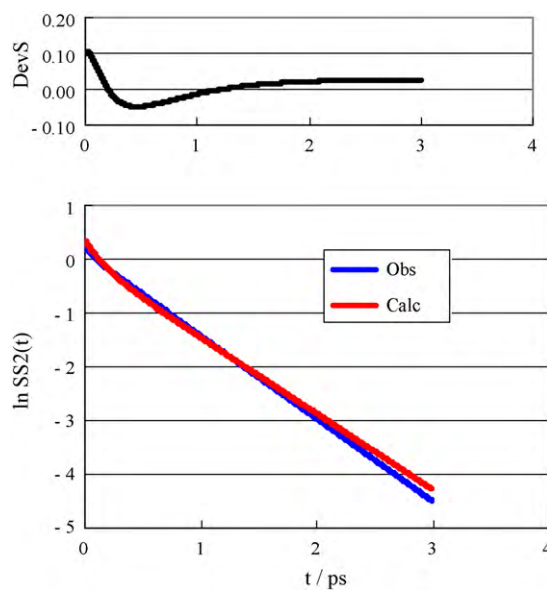


**Fig. 3.** TRSS of CA in water.  $SS_2(t)$  is described by Eq. (2) (unit kK). The observed TRSS was taken from Ref. [34].  $\mu_e$  and  $\varepsilon_c$  were varied so as to obtain the minimum value of  $\chi^2$ . The value of  $\chi^2$  was  $9.12 \times 10^{-4}$ . Upper panel shows deviation given by Eq. (4). See the legend of Fig. 2 for more information. Temperature was 295 K.



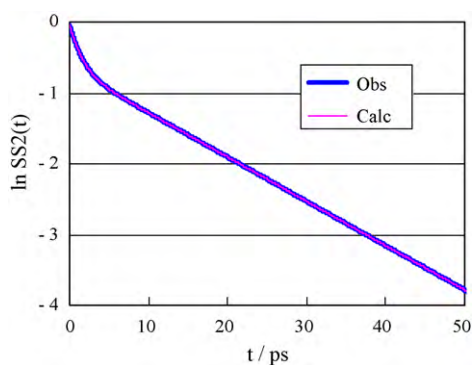


**Fig. 4.** Energy shift of Trp in monellin in water.  $SS_2(t)$  is specified as in Eq. (2) (unit in kK). The observed TRSS was taken from Ref. [25].  $\mu_e$ ,  $\varepsilon_0$ ,  $\varepsilon_1$ ,  $\varepsilon_c$ ,  $\tau_1$ ,  $\tau_2$ , and  $D_0$  were obtained by the best-fit procedure as described in Section 2.3, and listed in Table 2. The other physical constants are listed in Table S1. Temperature was 295 K.

### 3.3. TRSS of Trp and Lf in proteins

3-Methylindole was used as a substitute for Trp in proteins. Characteristics of 3-methylindole are listed in Table S1. First the observed TRSS data were analyzed with frequency-dependent dielectric constant with single relaxation time, but never obtained reasonable results. Then the data were analyzed with two relaxation times. In 2-relaxation time analysis  $\varepsilon_0$ ,  $\varepsilon_1$ ,  $\varepsilon_c$ ,  $D_0$ ,  $\mu_e$ ,  $\tau_1$ ,  $\tau_2$  were unknown parameters. The theoretical value was used as  $\mu_g$  listed in Table S1. Fig. 4 shows TRSS of Trp in native monellin. The observed data were taken from the results of Peon et al. [25]. Agreement between the observed and calculated  $SS_2(t)$  was excellent (the value of  $\chi^2$  was  $6.68 \times 10^{-17}$ ). Table 2 lists the determined parameters. The best-fit values were  $\varepsilon_0 = 78.4$ ,  $\varepsilon_1 = 6.47$ ,  $\varepsilon_c = 4.51$ ,  $D_0 = 1.86 \times 10^8 \text{ s}^{-1}$ ,  $\mu_e = 9.86 \text{ D}$ ,  $\tau_1 = 0.161 \text{ ns}$  and  $\tau_2 = 2.17 \text{ ps}$ .  $\varepsilon = 4$  was used for all systems. The values of  $g_2$  (0.9–0.96) of Trp in proteins were much greater than those of water (0.02–0.03, see Table S2). The Stokes shift,  $SS_2(0) - SS_2(\infty)$ , was 0.96 kK, which was the same as the experimental value [25]. The obtained decay constants of  $SS_2(t)$  were also the same as the experimental decay constants.

Fig. 5 shows TRSS of C<sub>1</sub> protein. Chromophore was assumed to be Lf. The experimental decay parameters were taken from the results by Chosrowjan et al. [34]. Agreement between the both  $SS_2(t)$  was again excellent with the value of  $\chi^2$  of  $4.64 \times 10^{-23}$ . The best-fit parameters in C<sub>1</sub> protein were  $\varepsilon_0 = 77.7$ ,  $\varepsilon_1 = 20.4$ ,  $\varepsilon_c = 8.36$ ,  $D_0 = 1.30 \times 10^5 \text{ s}^{-1}$ ,  $\mu_e = 23.0 \text{ D}$ ,  $\tau_1 = 0.912 \text{ ns}$  and  $\tau_2 = 1.91 \text{ ps}$ . These parameters together with those of denatured monellin and apomyoglobin are listed in Table 2.

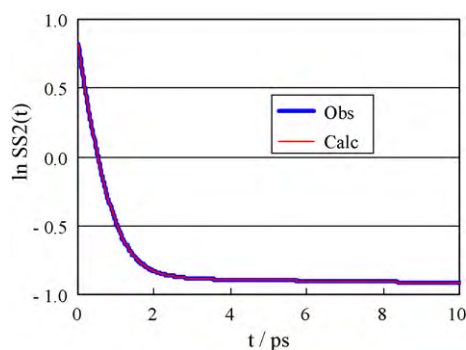


**Fig. 5.** TRSS of C<sub>1</sub> protein in water.  $SS_2(t)$  is described as in Eq. (2) (unit in kK). The observed TRSS was taken from Ref. [34]. The calculated TRSS was obtained using the best-fit parameters of  $\mu_e$ ,  $\tau_1$ ,  $\tau_2$ ,  $\varepsilon_0$ ,  $\varepsilon_1$ ,  $\varepsilon_c$ , and  $D_0$ , as in Fig. 4, and listed in Table 2. The value of  $\chi^2$  was  $4.64 \times 10^{-23}$ . The other physical constants used for the calculation are listed in Table S1.

Agreements between the observed and calculated decay constants in  $SS_2(t)$  and the amounts of the Stokes shift were striking in all systems. The values of  $\varepsilon_0$  were 73–78, which were similar to or a little smaller than that of water as listed in Table S2. The values of  $\varepsilon_c$  were ca. 5 in Trp in the proteins, and 8.4 in Lf of C<sub>1</sub> protein, which were much smaller than those of free fluorophores in water. Rotational diffusion coefficients of Trp in proteins and Lf in C<sub>1</sub> protein were in the range of  $10^5$ – $10^7 \text{ s}^{-1}$ , which were compared to those of free fluorophores in water,  $10^8$ – $10^9 \text{ s}^{-1}$ . The diffusion coefficient was least in the denatured monellin, suggesting that the indole ring is not free to rotate even though the protein is denatured. The values of  $\mu_e$  were 8–10 D in Trp of proteins, and 23 D in Lf in C<sub>1</sub> protein, which were much greater than the theoretical values of 3-methylindole, 5.73 D, and Lf in the excited states, 12.6 D in water. In the proteins ionic amino acids may exist near the fluorophores, causing the microenvironment to be different from water. The Stokes shift,  $SS_2(0) - SS_2(\infty)$ , of Lf in C<sub>1</sub> protein was 2.262 kK, while it was 0.5 kK in the Stokes shift of riboflavin tetrabutylate obtained under steady-state excitation [41]. The extraordinary large Stokes shift in C<sub>1</sub> protein compared to the one obtained in organic solvents was interpreted in terms of the presence of ionic amino acids in the protein [34].

The shorter relaxation times,  $\tau_1$ , were 2–10 ps, and the longer relaxation times,  $\tau_2$ , 0.2–0.9 ns in all systems. The fractions ( $g_1$ ) for  $\tau_1$  and  $g_2$  for  $\tau_2$  were 0.03–0.2, and 0.95–0.91, respectively.  $g_1$  (0.22) in C<sub>1</sub> protein was much greater than those of Trp in the proteins (0.03–0.1).  $\tau_2$  in the proteins was in the range of sub-nanoseconds while it was ps in water. Long tail of TRSS found in TRSS of fluorophores in proteins can be ascribed by the presence of  $\tau_2$  in sub-nanosecond time domain.

The observed TRSS data were also analyzed with three relaxation times in the frequency-dependent dielectric constant in Eq. (1). The obtained parameters were listed in Table 3. Agreements between the observed and calculated TRSS were excellent, but any improvements in  $\chi^2$  were not obtained, even two parameters ( $\varepsilon_2$  and  $\tau_3$ ) were added. Comparing to the results of the 2-relaxation time analysis (Table 2), the values of  $g_1$  obtained from 2- and 3-relaxation analyses were not different much, though  $\varepsilon_0$  were greater by 15–35 in the 3-relaxation time analysis. The values of the additional relaxation time ( $\tau_3$ ) were almost same with those of  $\tau_2$ , which suggests that two relaxation times are enough to describe the observed TRSS in proteins.

### 3.4. Comparison between MD model and continuum model for TRSS in proteins

It is very important to compare solvation dynamics of the chromophores in proteins between continuum and MD models. TRSS of proteins is often decomposed into three parts in MD model [33].

$$SS_M(t) = SS_W(t) + SS_{WP}(t) + SS_P(t) \quad (7)$$

W, WP, and P denote water, water–protein interface and protein, respectively. To compare continuum model with MD model, we use the results obtained by the 3-relaxation time analysis (see Table 3).

$$SS_C(t) = SS_1(t) + SS_2(t) + SS_3(t) \quad (8)$$

In the continuum model TRSS may be divided into three parts corresponding to contributions from  $\tau_1$ ,  $\tau_2$ , and  $\tau_3$ . Decay constants and amplitudes of  $SS_i(t)$  are  $\varphi_i$  and  $\alpha_i$  ( $i=1-3$ ), respectively. We assume that  $SS_1(t)$  is from water molecules almost freely mobile,  $SS_2(t)$  from water at the protein–water interface, and  $SS_3(t)$  from the protein part near a chromophore, though  $SS_2(t)$  and  $SS_3(t)$  could not be experimentally separated. Despite the similarity in magnitudes of  $\tau_2$  and  $\tau_3$ ,  $g_2$  (70–90%) was much greater than  $g_3$  (5%). Fig. 6 illustrates changes in TRSS of apomyoglobin as a function of  $\tau_2$  (Fig. 6A) or  $\tau_3$  (Fig. 6B). As the relaxation time became slower, TRSS

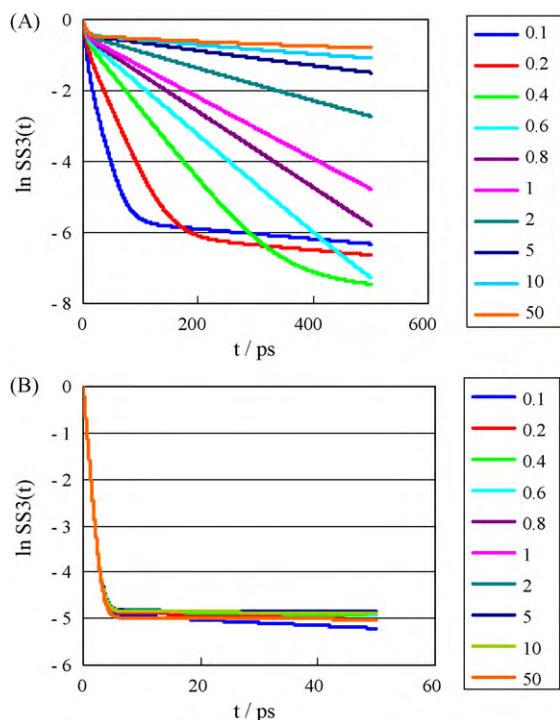


**Fig. 6.** Dependence of TRSS of apomyoglobin on the relaxation times. Panels A and B indicate dependencies of  $SS_3(t)$  on  $\tau_2$  and  $\tau_3$ , respectively. The inset in A shows the values of  $\tau_2$ , and in B shows those of  $\tau_3$ . According to the calculations the parameters other than  $\tau_2$  in A and  $\tau_3$  in B were kept constant, as listed in Table 3. At enough long  $\tau_2$ ,  $SS_3(t)$  in A apparently decayed with two phases with very short and long decay constants. In B the dependence of  $SS_3(t)$  on  $\tau_3$  was minimal. In both cases the slower components became flat when the responsible relaxation times were long enough.

changed drastically; at enough long  $\tau_2$  the slow component was going to be flat (no decay as in frozen state in MD model [30,32]). There still remained, however, a fast decaying component even at 50 ns of  $\tau_2$ . Fig. 6B shows dependence of  $SS_3(t)$  profile on  $\tau_3$ . The change in  $SS_3(t)$  as a function of  $\tau_3$  was minimal. Fig. 7 shows dependencies of amplitudes of  $\alpha_1$ ,  $\alpha_2$  and  $\alpha_3$ , and decay constants  $\varphi_1$ ,  $\varphi_2$ , and  $\varphi_3$  on  $\tau_2$ . Relationship between these observed decay constants and  $\tau_i$  ( $i=1-3$ ) are not straightforward (see Supplemental Material B). At the very short time range of  $\tau_2$ ,  $\alpha_1$  was dominant (the values of  $\varphi_1$  was around 5 ps and almost independent of  $\tau_2$ ), followed by  $\alpha_3$  and  $\alpha_2$ . According to the best fit in the natural state,  $\tau_2$  (0.878 ns),  $\alpha_3=0.63$  (corresponding to  $\alpha_2$  in Table 3),  $\alpha_1=0.37$ ,  $\alpha_2 \sim 0$ , were obtained. Fig. 7C and D show dependencies of the decay constants on  $\tau_2$ . The values of  $\varphi_2$  increased gradually in the short range of  $\tau_2$ , and then drastically above 5 ns of  $\tau_2$ . The values of  $\varphi_3$  slightly increased from 0.7 ns to 8 ns as  $\tau_2$  increased from 0.1 ns to 50 ns. These results in Figs. 6 and 7 suggest that the slow component becomes flat when the protein part or the water–protein interface is frozen. This behavior of TRSS in continuum model is similar with the freezing state obtained by MD model [30,32].

#### 4. Discussion

$\varepsilon_c$  was first introduced into the theoretical expression of TRSS by Bagchi et al. [3], and subsequently  $\varepsilon_c$  was considered to be optical dielectric constant of solute in the ground state [1,2,16,17], according to Bättcher [40]. In the present work  $\varepsilon_c$  was interpreted to be dielectric constant of solute in the excited state. Agreement between the observed and calculated TRSS in water was very good in free Trp according to Model B [37], and quite good in CA according to Model D [39].

The molecular mechanism of underlying slow relaxation processes of chromophores in proteins near the protein–water surfaces has been investigated by several groups, using MD model. Bagchi and Zewail group [20–26] proposed a mechanism in which water

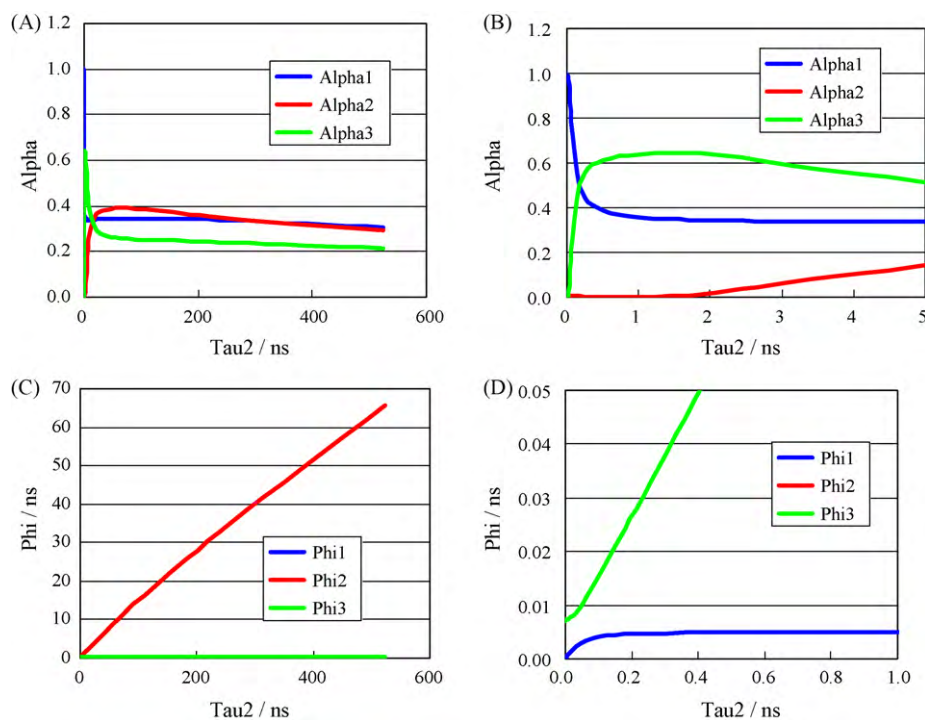


**Fig. 7.** Dependencies of  $\alpha$  and  $\varphi$  of Trp in apomyoglobin on  $\tau_2$ . (A)  $\alpha$  in the long time region of  $\tau_2$ . (B)  $\alpha$  in the short time region of  $\tau_2$ . (C)  $\varphi$  in the long time region of  $\tau_2$ . (D)  $\varphi$  in the short time region of  $\tau_2$ . Alpha1, Alpha2 and Alpha3 in the inserts of A and B denote  $\alpha_1$ ,  $\alpha_2$  and  $\alpha_3$ , respectively. Phi1, Phi2 and Phi3 in the inserts of C and D denote  $\varphi_1$ ,  $\varphi_2$ , and  $\varphi_3$ , respectively. The other parameters are listed in Table 3. Meanings of  $\alpha$ 's and  $\varphi$ 's are described at footnotes in Table 3.

**Table 3**  
Best-fit parameters of proteins obtained with three relaxation times<sup>a</sup>.

System (fluorophore)	Best-fit parameter										$\chi^2$ <sup>d</sup> ( $\times 10^{-17}$ )		
	$\varepsilon_0$	$\varepsilon_1$	$\varepsilon_2$	$\varepsilon_c$	$D_0$ ( $\mu\text{s}^{-1}$ )	$\mu_e$ (D)	$\tau_1$ (ps) ( $g_1$ )	$\tau_2$ (ns) ( $g_2$ )	$\tau_3$ (ns) ( $g_3$ )	SS <sub>3</sub> (0) – SS <sub>3</sub> ( $\infty$ ) (kK)		$\varphi_1$ <sup>b</sup> (ps) ( $\alpha_1$ %)	$\varphi_2$ <sup>b</sup> (ps) ( $\alpha_2$ %)
Native monellin (3-methylindole)	93.2	12.4	8.02	23.6	9.70	5.63	2.12 (0.049)	0.122 (0.905)	0.122 (0.045)	0.960	1.30 (0.46)	16.0 (0.54)	1.89
Denatured monellin (3-methylindole)	101	20.9	9.61	23.0	3.85	5.67	9.56 (0.116)	0.282 (0.826)	0.284 (0.058)	0.960	3.5 (0.72)	56.0 (0.28)	4.08
Apomyoglobin (3-methylindole)	92.4	12.4	9.03	23.4	4.21	7.39	7.36 (0.038)	0.739 (0.905)	0.746 (0.057)	0.660	5.0 (0.367)	87.0 (0.633)	0.283
C1 protein (LF)	115	34.6	9.04	30.5	7.65	15.4	1.88 (0.231)	0.878 (0.724)	0.925 (0.046)	2.262	0.455 (0.816)	250 (0.184)	166

<sup>a</sup> The experimental data are shown in Table 2.

<sup>b</sup> The calculated decay constants of TRSS.

<sup>c</sup> The calculated amplitudes of TRSS.

<sup>d</sup>  $\chi^2$  given by Eq. (6).

molecules near the fluorophores both without much motional freedom at the interface and with the partial freedom in the hydrated layer are responsible for the slow components. According to their model, the observed slow dynamics is directly related to water residence times at the sites, and dynamic exchange of water molecules is important between the bound and “quasi-free” water molecules. Nilsson and Halle [27] concluded that the slow decay is closely related to protein dynamics near the chromophore, and a collective motion of the water molecules at the hydrated layer is important. Li et al. [30,32] have found that when either of protein or water molecules is frozen, the slow component disappeared. They also emphasized that the slow component results from strongly coupled protein–water motions, and requires protein flexibility.

Agreement between the observed and calculated TRSS of proteins investigated using the continuum model were all excellent, while MD calculations always give much greater fractions of TRSS with faster decay constants both in free Trp and Trp in proteins. The fractions of TRSS with faster and slower decay constants of free Trp obtained by MD [27] were 0.86 with the decay constant, 0.07 ps, and 0.14 with 0.7 ps, respectively, while the experimental values [25,35] were 0.2 with 0.18 ps and 0.8 with 1.11 ps (see Table 1), respectively. In native monellin the decay parameters of Trp3 obtained by MD were 0.66 with 0.07 ps and 0.22 with 1 ps and 0.12 with 23 ps, while the experimental values were 0.46 with 1.3 ps and 0.54 with 16 ps (see Table 2) [25]. Li et al. [30] also reported that total Stokes shift in both isomers of Trp in apomyoglobin obtained by non-equilibrium MD was 17.7–22.5 kJ/mol, while 7.9 kJ/mol by experiment, and further no faster decay within 1 ps was observed in the experiment, but more than 50% of the total Stokes shift was obtained in this time domain of the simulations.

The values of  $\varepsilon_0$  in the proteins were close to one of water, and  $\tau_1$  close to free water. It is reasonably assigned this component as freely mobile water molecules near the chromophores. Fraction  $g_1$  was 4–12% in Trp and 23% in Iso. In C1 accessibility of Iso to freely mobile water molecules may be quite great. Though in the natural state  $\tau_2$  and  $\tau_3$  were similar, the values of  $g_2$  (72–91%) were much greater than those of  $g_3$  (5–6%). If we consider that such great Stokes shift has never taken place when a chromophore is buried inside a protein, it is not unreasonable to assign the dominant component with  $\tau_2$  is from water molecules at the interface, then  $\tau_3$  from the protein part. In the present physical picture of the Stokes shift in proteins, motions of water molecules at the interface may be cooperative with those of amino acids near the chromophores, because the values of  $\tau_2$  and  $\tau_3$  were similar. This is in accordance with a model by Halle and Nilsson [33].

According to the model by Halle and Nilsson [33] Stokes shift comes from the water–protein interface with effective permittivity  $\varepsilon$  which is different from  $\varepsilon_0$  of water, and is divided into two parts, as in Eq. (9).

$$\Delta E = \Delta E_p + \Delta E_w \quad (9)$$

Here  $\Delta E_p$  is Coulomb interaction energy between a chromophore and nearby amino acids, and  $\Delta E_w$  is the energy between the chromophore and water molecules at the interface. They assumed that  $\Delta E = \Delta E_p/\varepsilon$ , and

$$\Delta E_w = \Delta E - \Delta E_p = -\left(1 - \frac{1}{\varepsilon}\right) \Delta E_p \quad (10)$$

Namely,  $\Delta E_p$  and  $\Delta E_w$  are not independent in Eq. (9). Eq. (10) was extended to the slow component of TRSS in proteins.

$$SS_w(t) = -\left(1 - \frac{1}{\varepsilon}\right) SS_p(t) \quad (11)$$

Eq. (11) indicates that  $SS_w(t)$  and  $SS_p(t)$  are not independent, neither of them is frozen (at infinite relaxation time), and the slow decaying component disappears. When the whole slow decaying

TRSS is considered,  $SS(t) = SS_p(t)$  where there is no contribution from water molecules at the interface to  $SS(t)$ . This scenario does not seem to be reasonable, because  $\varepsilon$  is different from  $\varepsilon_0$ , and accordingly, each water molecule is considered as a solute, and therefore, the interaction at the interface with dielectric constant  $\varepsilon$  between the chromophore and each water molecule must be explicitly taken into account. According to the model by Halle and Nilsson [33], the slow decay in TRSS arises from the polarization of the solvent induced by the time-dependent electric field from the probe and protein charges. The fast decay is originated by very slight orientational preferences among a large number of water molecules, within and beyond the hydration layer in a time scale of a few picoseconds.

We propose Eq. (12) instead of Eq. (9).

$$\Delta E = \frac{\Delta E_W + \Delta E_P}{\varepsilon} \quad (12)$$

In Eq. (12)  $\Delta E_W$  and  $\Delta E_P$  are independent, and specify the energy of water molecules at the interface with the relaxation time of  $\tau_2$ , and of flexible protein part near the chromophore with  $\tau_3$ , respectively. Eq. (12) is a simplified model for our method using 3-relaxation time analysis. With this model the frozen state of protein or water molecules at the interface was also consistent with a long relaxation time. Our model is in accordance with one given by Halle and Nilsson [33] in the natural state, which claims that  $\Delta E_W$  is dependent (cooperative) on  $\Delta E_P$ , because the magnitudes of  $\tau_2$  and  $\tau_3$  are similar. However, the both models should be different at extreme conditions as in the frozen state.

Recently, Jesenska et al. [42] have reported that TRSS of DbjA from *Bradyrhizobium japonicum* USDA11019 and DhaA from *Rhodococcus rhodochrous* NCIMB13064 decay in sub-nanoseconds and several nanosecond time domains, not in the picosecond domain. Time-resolution of their instrumental system, however, is not high enough to observe sub-picosecond decays of TRSS. Accordingly, the presence of fast decay components of TRSS in these protein systems is not clear.

#### Appendix A. Supplementary data

Supplementary data associated with this article can be found, in the online version, at doi:10.1016/j.jphotochem.2010.07.018.

#### References

- [1] E. Lippert, Z. Naturforsch. 10a (1955) 541.
- [2] N. Mataga, Y. Kaifu, M. Koizumi, Bull. Chem. Soc. Jpn. 28 (1955) 690.
- [3] B. Bagchi, D.W. Oxytoby, G.R. Fleming, Chem. Phys. 86 (1984) 257.
- [4] E.W. Castner Jr., G.R. Fleming, B. Bagchi, Chem. Phys. Lett. 143 (1988) 270.
- [5] G. Fleming, Chemical Applications of Ultrafast Spectroscopy, Oxford University Press, Oxford, 1986 (Chapter 6).
- [6] M. Maroncelli, G.R. Fleming, J. Chem. Phys. 86 (1987) 6221.
- [7] M. Maroncelli, J. McInnes, G.R. Fleming, Science 247 (1989) 1674.
- [8] P.F. Barbara, W. Jarzeba, Adv. Photochem. 15 (1990) 1.
- [9] W. Jarzeba, G.C. Walker, A.E. Johnson, P.F. Barbara, Chem. Phys. 152 (1991) 57.
- [10] R. Jimenez, G.R. Fleming, P.V. Kumar, M. Maroncelli, Nature 369 (1994) 471.
- [11] G.R. Fleming, M. Cho, Annu. Rev. Phys. Chem. 47 (1996) 109.
- [12] A. Papazyan, M. Maroncelli, J. Chem. Phys. 102 (1995) 2888.
- [13] P.V. Kumar, M. Maroncelli, J. Chem. Phys. 103 (1995) 3038.
- [14] B. Brown, J. Chem. Phys. 102 (1995) 9059.
- [15] T.-W. Nee, R. Zwentig, J. Chem. Phys. 52 (1970) 6353.
- [16] F. Tanaka, N. Mataga, Chem. Phys. 236 (1998) 277.
- [17] N. Tamai, T. Nomoto, F. Tanaka, Y. Hirata, T. Okada, J. Phys. Chem. A 106 (2002).
- [18] D.W. Pierce, S.G. Boxer, Biophys. J. 68 (1995) 1583.
- [19] X.J. Jordinades, M.J. Lang, X. Song, G.R. Fleming, J. Phys. Chem. B 103 (1999) 7995.
- [20] N. Nandi, K. Bhattacharyya, B. Bagchi, Chem. Rev. 100 (2000) 2013.
- [21] B. Bagchi, Chem. Rev. 105 (9) (2005) 3197.
- [22] K. Bhattacharyya, Acc. Chem. Res. 36 (2003) 95.
- [23] S.K. Pal, J. Peon, A.H. Zewail, Proc. Natl. Acad. Sci. U.S.A. 99 (2002) (1763).
- [24] S.K. Pal, J. Peon, B. Bagchi, A. Zewail, J. Phys. Chem. B 106 (2002) 12376.
- [25] J. Peon, S. Kumar, A.H. Zewail, Proc. Natl. Acad. Sci. U.S.A. 99 (2002) 10964.
- [26] J.K.A. Kamal, L. Zhao, A. Zewail, Proc. Natl. Acad. Sci. U.S.A. 101 (2004) 13411.
- [27] L. Nilsson, B. Halle, Proc. Natl. Acad. Sci. U.S.A. 102 (2005) 13867.
- [28] J. Xu, D. Topygin, K.J. Graver, R.A. Albertini, R.S. Savtchenko, N.D. Meadow, S. Roseman, P.R. Callis, L. Brand, J.R. Knutson, J. Am. Chem. Soc. 28 (2006) 1214.
- [29] L. Zhang, Y.-T. Kao, W. Qiu, L. Wang, D. Zhong, J. Phys. Chem. B 110 (2006) 18097.
- [30] T. Li, A.A. Hassanari, Y.-T. Kao, D. Zhong, S.J. Singer, J. Am. Chem. Soc. 29 (2007) 3376.
- [31] A.A. Golosov, M. Karplus, J. Phys. Chem. B 111 (2007) 1482.
- [32] T. Li, A.A. Hassanali, S.J. Singer, J. Phys. Chem. B 112 (2008) 16121.
- [33] B. Halle, L. Nilsson, J. Phys. Chem. B 113 (2009) 8210.
- [34] H. Chosrowjan, S. Taniguchi, N. Mataga, T. Phongsak, J. Sucharitakul, P. Chaiyen, F. Tanaka, J. Phys. Chem. B 113 (2009) 8439 (Letter).
- [35] X. Shen, J.R. Knutson, J. Phys. Chem. B 105 (2001) 6260.
- [36] A. Beneduci, J. Mol. Liq. 138 (2007) 55.
- [37] J.T. Kindt, C.A. Schmittenmaer, J. Phys. Chem. 100 (1996) 10373.
- [38] J. Bartel, K. Bachhumber, R. Buchner, H. Hetzenauer, Chem. Phys. Lett. 165 (1990) 369.
- [39] M.L.T. Asaki, A. Redondo, T.A. Zawodzinski, A.J. Taylor, J. Chem. Phys. 116 (2002) 8470.
- [40] C.J.F. Böttcher, Theory of Electric Polarization, vol. 1, Elsevier, Amsterdam, 1973, p. 186.
- [41] A. Kotaki, K. Yagi, J. Biochem. (Tokyo) 68 (1970) 509.
- [42] A. Jesenska, J. Sýkora, A. Olžýňská, J. Brezovsky, Z. Zdráhal, J. Damborský, M. Hof, J. Am. Chem. Soc. 131 (2009) 494–501.